Biological Psychiatry

Archival Report

Maternal Immune Activation Delays Excitatory-to-Inhibitory Gamma-Aminobutyric Acid Switch in Offspring

Irene Corradini, Elisa Focchi, Marco Rasile, Raffaella Morini, Genni Desiato, Romana Tomasoni, Michela Lizier, Elsa Ghirardini, Riccardo Fesce, Diego Morone, Isabella Barajon, Flavia Antonucci, Davide Pozzi, and Michela Matteoli

ABSTRACT

BACKGROUND: The association between maternal infection and neurodevelopmental defects in progeny is well established, although the biological mechanisms and the pathogenic trajectories involved have not been defined.

METHODS: Pregnant dams were injected intraperitoneally at gestational day 9 with polyinosinic:polycytidylic acid. Neuronal development was assessed by means of electrophysiological, optical, and biochemical analyses.

RESULTS: Prenatal exposure to polyinosinic:polycytidylic acid causes an imbalanced expression of the Na^+-K^+-$2Cl^-$ cotransporter 1 and the K^+-Cl^- cotransporter 2 (KCC2). This results in delayed gamma-aminobutyric acid switch and higher susceptibility to seizures, which endures up to adulthood. Chromatin immunoprecipitation experiments reveal increased binding of the repressor factor RE1-silencing transcription (also known as neuron-restrictive silencer factor) to position 509 of the KCC2 promoter that leads to downregulation of KCC2 transcription in prenatally exposed offspring. Interleukin-1 receptor type I knockout mice, which display braked immune response and no brain cytokine elevation upon maternal immune activation, do not display KCC2/Na^+-K^+-$2Cl^-$ cotransporter 1 imbalance when implanted in a wild-type dam and prenatally exposed. Notably, pretreatment of pregnant dams with magnesium sulfate is sufficient to prevent the early inflammatory state and the delay in excitatory-to-inhibitory switch associated to maternal immune activation.

CONCLUSIONS: We provide evidence that maternal immune activation hits a key neurodevelopmental process, the excitatory-to-inhibitory gamma-aminobutyric acid switch; defects in this switch have been unequivocally linked to diseases such as autism spectrum disorder or epilepsy. These data open the avenue for a safe pharmacological treatment that may prevent the neurodevelopmental defects caused by prenatal immune activation in a specific pregnancy time window.

Keywords: Epilepsy, GABA switch, KCC2, Maternal immune activation

https://doi.org/10.1016/j.biopsych.2017.09.030

Disruption of correct neurodevelopmental trajectories by maternal immune activation (MIA) is a critical factor in the development of neurological and neuropsychiatric disorders (1–3), especially when maternal infections synergize with a susceptible genetic background or when the prenatal event is followed by postnatal risk factors that act as "second hits" (3,4).

In recent years, the consequences of maternal infections on offspring brain have been explored using mouse models based on prenatal exposure to immune stimuli (5–9). The immunogens most commonly used in rodent models have been lipopolysaccharide, a component of the cell wall of gram-negative bacteria that binds to toll-like receptor 4 and mimics bacterial infection, or polyinosinic:polycytidylic acid (PolyI:C), a double-stranded, synthetic RNA that binds to toll-like receptor 3 like viral nucleic acid. Injection of either immunogen initiates a signaling cascade that leads to the production of inflammatory mediators, such as chemokines, cytokines, and complement proteins (10).

Consistent with epidemiological data, preclinical studies in these models have shown a wide spectrum of long-term behavioral changes, including impaired sensorimotor gating (prepulse inhibition) (8,11,12), increased anxiety-like behavior (13), cognitive deficits (12,14), and altered exploratory behavior (6,12). The phenotypic abnormalities in offspring are frequently accompanied by brain alterations, although with a high degree of variability depending on the specific immune activation paradigm (7,15,16). Injecting the immunogen at different time points during gestation leads to different neuropathological features (6), gene expression profiles (7), and behavioral abnormalities in offspring (6).

Although epidemiological and preclinical evidence indicate that intrauterine exposures elicit enduring effects on offspring,

ISSN: 0006-3223

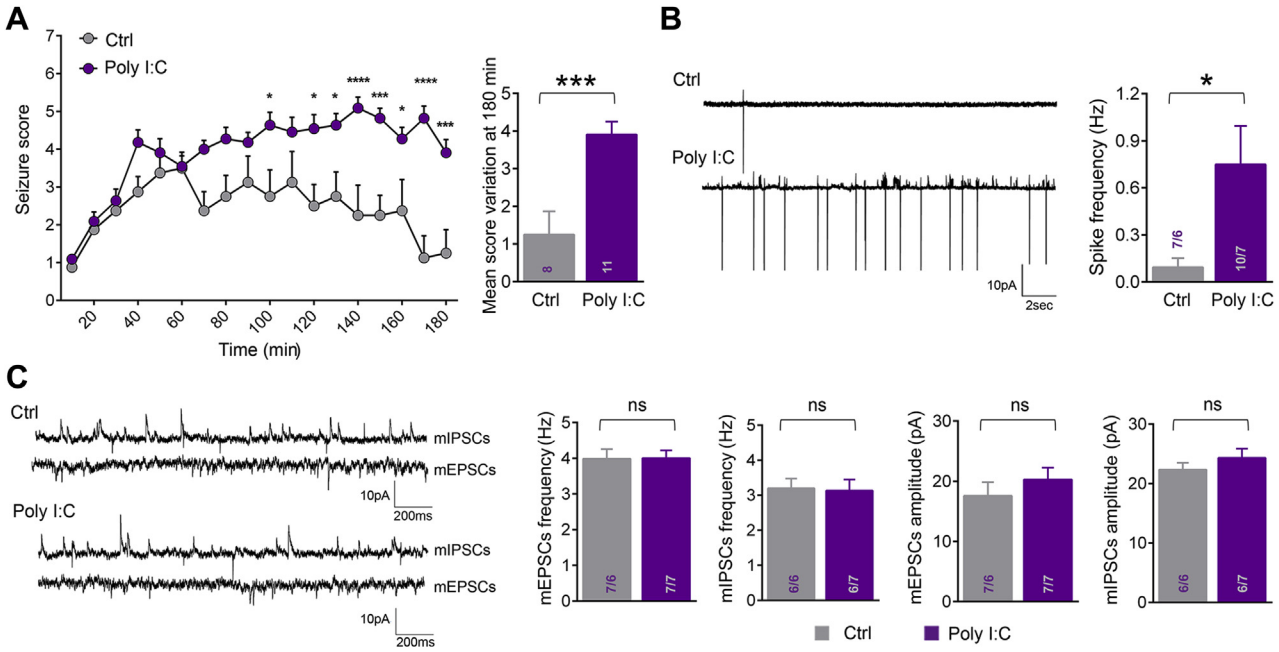

Figure 1. Maternal immune activation results in altered network activity and increased offspring susceptibility to seizures in the absence of synaptic modifications. **(A)** (Left) Evaluation of the behavioral response of control (Ctrl) mice and mice that were prenatally treated with polyinosinic:polycytidylic acid (PolyI:C) to 35 mg/kg kainic acid systemic injection. All mice were scored every 10 minutes over a 3-hour period. In all mice, kainate injection resulted in immobility and staring during the first 10 minutes. PolyI:C mice showed clear signs of focal epilepsy (head bobbing), culminating in continuous generalized seizures (stage 5, status epilepticus) that lasted for about 80 minutes. Two-way analysis of variance followed by Sidak's multiple comparisons test, $^{*}p < .05$, $^{***}p < .001$, $^{****}p < .0001$. (Right) Quantitative analysis of the mean score variation at 180 minutes. Student's *t* test, $^{***}p < .001$. Numbers in bars indicate the number of animals. **(B)** (Left) Representative electrophysiological traces of cell-attached recording in acute cortical slices at postnatal day 20 established from PolyI:C and Ctrl mice. (Right) Quantitative analysis of the spiking activity. Bars represent mean ± SEM (Ctrl = 0.09 ± 0.06, PolyI:C = 0.75 ± 0.24). Mann-Whitney *U* test, $^{*}p < .05$. Numbers in bars indicate the number of cells/animals. **(C)** (Left) Representative traces of excitatory and inhibitory miniature postsynaptic currents recorded from postnatal day 20 cortical slices obtained from PolyI:C prenatally treated mice (lower traces) and Ctrl mice (upper traces). (Right) Electrophysiological analysis of the frequency and the amplitude of miniature excitatory postsynaptic currents (mEPSCs) and miniature inhibitory postsynaptic currents (mIPSCs). Bars represent mean ± SEM (mEPSC frequency: Ctrl = 3.99 ± 0.27, PolyI:C = 4.01 ± 0.22; mIPSC frequency: Ctrl = 3.20 ± 0.27, PolyI:C = 3.13 ± 0.32; mEPSC amplitude: Ctrl = 17.57 ± 2.26, PolyI:C = 20.29 ± 1.98; mIPSC amplitude: Ctrl = 22.33 ± 1.14, PolyI:C = 24.33 ± 1.54). Student's *t* test. Numbers in bars indicate the number of cells/animals. ns, not significant.

the specific molecular targets and the pathogenic pathways involved in brain alterations after prenatal immune activation are still far from elucidated. Recent studies investigated possible alterations in offspring brain transcriptome or proteome, in the attempt to identify mechanisms at the basis of postnatal changes induced by MIA: a widespread dysregulation has been unveiled in several genes linked to neuronal development, mitochondrial function, synaptic vesicle recycling, cytoskeletal structures, energy metabolism, and signal transduction (17,18). However, the possible functional impact of these transcriptomic or proteomic changes is still unknown.

In this framework, we aimed to assess whether prenatal immune activation impacts synapse formation and function, and whether it affects the excitatory versus inhibitory balance in neurotransmission, which is one common trait shared by different neurodevelopmental diseases.

METHODS AND MATERIALS

Animals

All experiments followed the guidelines established by the European Directive 2010/63/EU and the Italian Governing Law 26/2014. Dams were injected with PolyI:C (Sigma-Aldrich, St. Louis, MO) or vehicle intraperitoneally on gestational day 9 (GD9). For the embryo transfer procedure, embryos from interleukin-1 receptor type I knockout (IL-1RI KO) female mice were implanted into wild-type (WT) pseudopregnant female mice, following standard techniques (19). The magnesium treatment protocol was adapted from Hallak *et al.* (20). Kainate treatment was performed as previously described (21), and seizure severity was determined according to Racine's scale (22).

Cell Cultures

Cortical neurons were established from C57BL/6 mice at embryonic day 18 (E18) from vehicle or PolyI:C-treated mothers as previously described (23,24).

Imaging and Electrophysiology

Calcium imaging was performed on cortical cultures as previously described (25,26).

Cultured cortical neurons were recorded at 14 days in vitro (DIV) using an Axopatch 200B amplifier with a Digidata 1440 digitizer (Axon Instruments, Foster City, CA). Whole cell recordings were performed as previously reported (25).

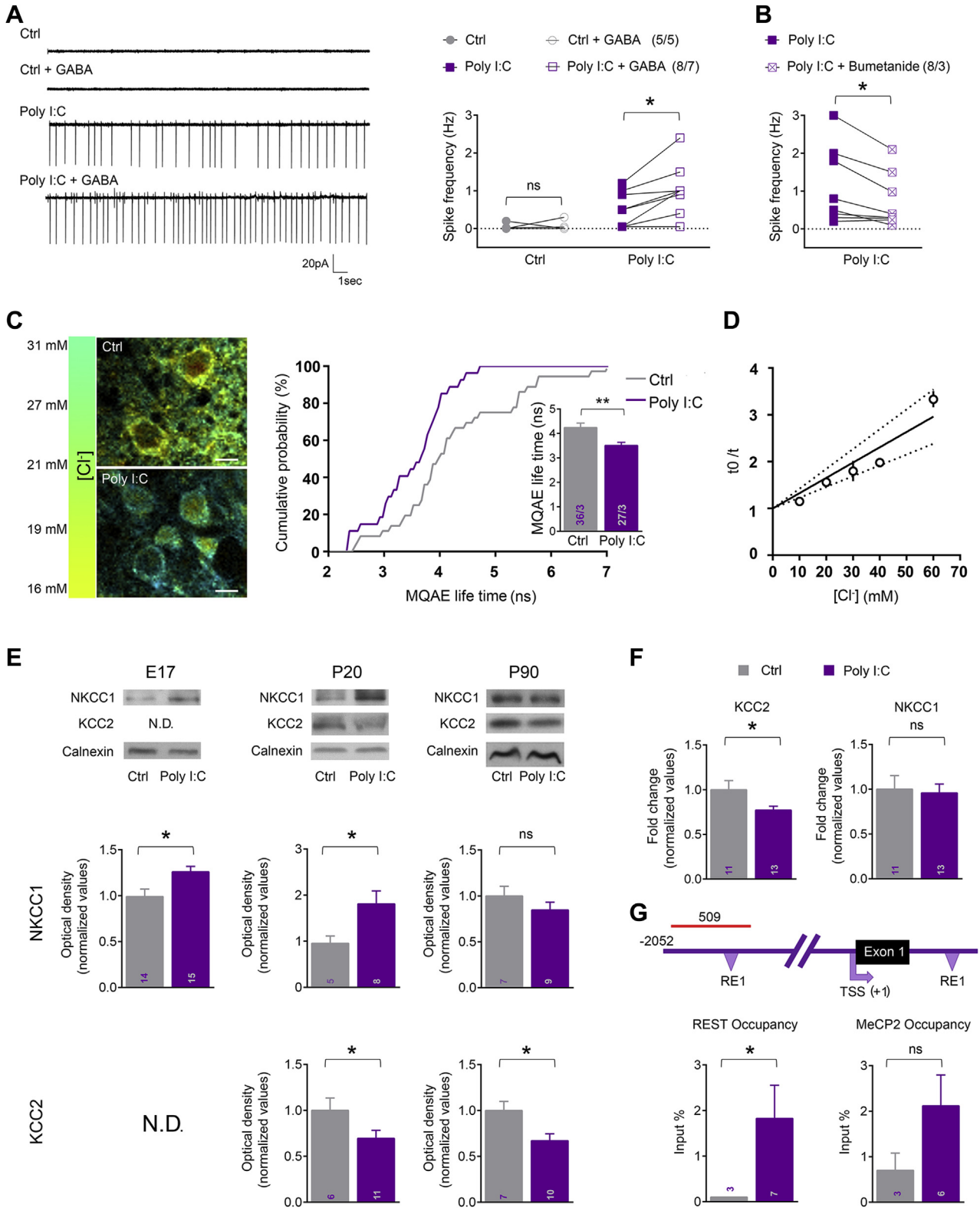
A
Ctrl
Ctrl + GABA
Poly I:C
Poly I:C + GABA
20pA
1sec
Ctrl
Ctrl + GABA (5/5)
Poly I:C
Poly I:C + GABA (8/7)
Spike frequency (Hz)
ns
*
Ctrl
Poly I:C
B
Poly I:C
Poly I:C + Bumetanide (8/3)
Spike frequency (Hz)
*
Poly I:C
C
31 mM
27 mM
21 mM
19 mM
16 mM
[Cl-]
Ctrl
Poly I:C
Cumulative probability (%)
MQAE life time (ns)
Ctrl
Poly I:C
**
MQAE life time (ns)
36/3
27/3
Ctrl
Poly I:C
D
t0 /t
[Cl-] (mM)
E
E17
P20
P90
NKCC1
KCC2
Calnexin
N.D.
Ctrl
Poly I:C
NKCC1
KCC2
Optical density (normalized values)
*
ns
14
15
5
8
7
9
6
11
7
10
F
Ctrl
Poly I:C
KCC2
NKCC1
Fold change (normalized values)
*
ns
11
13
G
509
-2052
Exon 1
RE1
TSS (+1)
RE1
REST Occupancy
MeCP2 Occupancy
Input %
*
ns
3
7
3
6

Electrophysiological recording from brain slices was performed as described by Lien *et al.* (27).

Biochemistry

Western blot analysis was performed on cortical tissues from E17, postnatal day 20 (P20), and P90 PolyI:C or vehicle prenatally treated mice and on 7 DIV cortical neurons.

Chromatin Immunoprecipitation and Real-time Polymerase Chain Reaction

Immunoprecipitation was performed on cortical tissue from P20 mice incubated with protein G Dynabeads (Invitrogen Corporation, Carlsbad, CA) bound to RE1-silencing transcription factor (REST) (Millipore, Burlington, MA) or methyl-CpG-binding protein 2 (Sigma-Aldrich) polyclonal antibody; K^+-Cl^- cotransporter 2 (KCC2) promoter was then analyzed by quantitative real-time polymerase chain reaction (PCR). For total RNA analysis, real-time PCR was performed on embryonic or P20 tissues.

Statistics

The results are presented as mean ± SEM. Student's two-tailed paired or unpaired *t* tests and one- or two-way analysis of variance, followed by Tukey's or Sidak's multiple comparisons test, were used for normal distributions. The Mann-Whitney nonparametric *U* test was used for non-normally distributed data.

Details can be found in the Supplement.

RESULTS

PolyI:C Mice Show Increased Susceptibility to Epilepsy in the Absence of Chronic Inflammation or Synaptic Alterations

A single PolyI:C exposure performed at GD9 (i.e., at the beginning of cortical neuronal layering) was sufficient to increase offspring susceptibility to seizures at 3 months of age. Response to intraperitoneal administration of 35 mg/kg kainic acid (KA) was compared in offspring of mothers exposed to PolyI:C versus vehicle (control), by behavioral evaluation repeated every 10 minutes over a 3-hour period (Figure 1A). In all mice, KA resulted in immobility and staring followed by head bobbing and isolated limbic motor seizures (Racine scale, stage 4), characterized by forelimb clonus and rearing. While control mice only displayed isolated limbic motor seizures, PolyI:C mice rapidly progressed to stage 5 (status epilepticus) and showed continuous generalized activity lasting for about 80 minutes (Figure 1A, left). One hundred eighty minutes after KA injection, PolyI:C mice still displayed a significantly higher mean Racine score relative to control mice (Figure 1A, right). PolyI:C mice did not display seizures either during normal activity or upon manipulation at any age; seizures were only evident after KA treatment. Contrary to prenatal exposure to the inflammatory hit, adult exposure did not result in any long-lasting increase of circuit hyperactivity. Indeed, a single PolyI:C treatment in adult mice failed to increase susceptibility to seizures (Supplemental Figure S1B). In line with the higher susceptibility to seizures, layer 5 neurons recorded by cell-attached patch clamp in acute cortical slices of PolyI:C-exposed progeny displayed a higher spike frequency than controls (Figure 1B).

Epilepsy may be the consequence of inflammatory processes (28), and therefore we investigated whether the hyperactivity and increased susceptibility to epilepsy observed in mice that were prenatally exposed to PolyI:C was associated with enhanced brain inflammation. Brains of 3-month-old mice that were prenatally exposed to either PolyI:C or vehicle were examined by confocal microscopy; the number and morphological appearance of microglial cells and the expression of proinflammatory markers were quantified. No differences were observed between PolyI:C and control mice, either in the number of microglia—revealed by the specific marker Iba1 (Supplemental Figure S2A)—or in the expression of CD11b (Supplemental Figure S2A) or glial fibrillary acidic protein (Supplemental Figure S2C). Unlike activated microglia, which are known to retract their branches and assume an

Figure 2. Polyinosinic:polycytidylic acid (PolyI:C) delays the excitatory-to-inhibitory gamma-aminobutyric acid (GABA) switch by increasing repressor factor RE1-silencing transcription factor (REST) (also known as neuron-restrictive silencer factor) binding to K^+-Cl^- cotransporter 2 (KCC2) promoter and reducing its transcription. **(A)** (Left) Representative traces of spontaneous spiking activity recorded in cell-attached patch-clamp configuration in acute slices from PolyI:C and control (Ctrl) mice before and after puff application of 200 μM GABA. (Right) Quantitative analysis of the spontaneous activity in cortical slices upon GABA application. Paired *t* test, $^*p < .05$. Numbers in brackets indicate the number of cells/animals. **(B)** Quantitative analysis of neuronal activity in cortical slices upon application of 10 μM bumetanide showed a significant reduction of spike frequency in PolyI:C slices. Paired *t* test, $^*p < .05$. Numbers in brackets indicate the number of cells/animals. **(C)** (Left) Representative images of two-photon imaging of fluorescence lifetime imaging microscopy values of $[Cl^-]_i$ in cortical neurons loaded with the chloride-sensitive dye *N*-(ethoxycarbonylmethyl)-6-methoxyquinolinium bromide (MQAE). $[Cl^-]_i$ is inversely proportional to the fluorescence lifetime imaging microscopy value of the dye. (Right) Cumulative probability and quantitative analysis of fluorescence lifetime imaging microscopy in PolyI:C and Ctrl cortical neurons show a significantly higher fraction of neurons displaying increased $[Cl^-]_i$ in PolyI:C cortical slice neurons compared with Ctrls. Bars represent mean ± SEM (Ctrl = 4.24 ± 0.18, PolyI:C = 3.51 ± 0.12). Student's *t* test, $^{**}p < .01$. Numbers in bars indicate the number of cells/animals (scale bar = 20 μm). **(D)** Stern–Volmer plot of MQAE quenching at a given Cl^- concentration allows for the determination of intracellular chloride concentration. The slope of the regression line gives a Stern–Volmer constant of $31M^{-1}$. **(E)** Representative Western blot lanes and biochemical analyses of ion cotransporter expression at different ages in cortices from PolyI:C and Ctrl offspring. (Bottom) KCC2 protein levels are significantly reduced in postnatal day 20 (P20) and P90 homogenates from mice prenatally treated with PolyI:C compared with Ctrls, while Na^+-K^+-$2Cl^-$ cotransporter 1 (NKCC1) protein levels (top) are significantly increased in embryonic day 17 (E17) and P20 cortical homogenates from PolyI:C mice compared with Ctrls and return to Ctrl levels in P90 cortices. Protein levels were normalized on either calnexin or tubulin. Student's *t* test, $^*p < .05$. Numbers in bars indicate the number of animals. **(F)** Real-time polymerase chain reaction analysis for ion cotransporters KCC2 and NKCC1 performed in P20 brains of PolyI:C- and vehicle-treated offspring. A significant reduction of messenger RNA levels was detected for KCC2 but not for NKCC1. **(G)** (Top) Map of the mouse *Kcc2* promoter. (Bottom) Chromatin immunoprecipitation assay for REST and methyl-CpG-binding protein 2 (MeCP2) binding to the *Kcc2* promoter showing an increased binding of both the transcription factors to position 509. N.D., not detectable; ns, not significant; TSS, transcription start site.

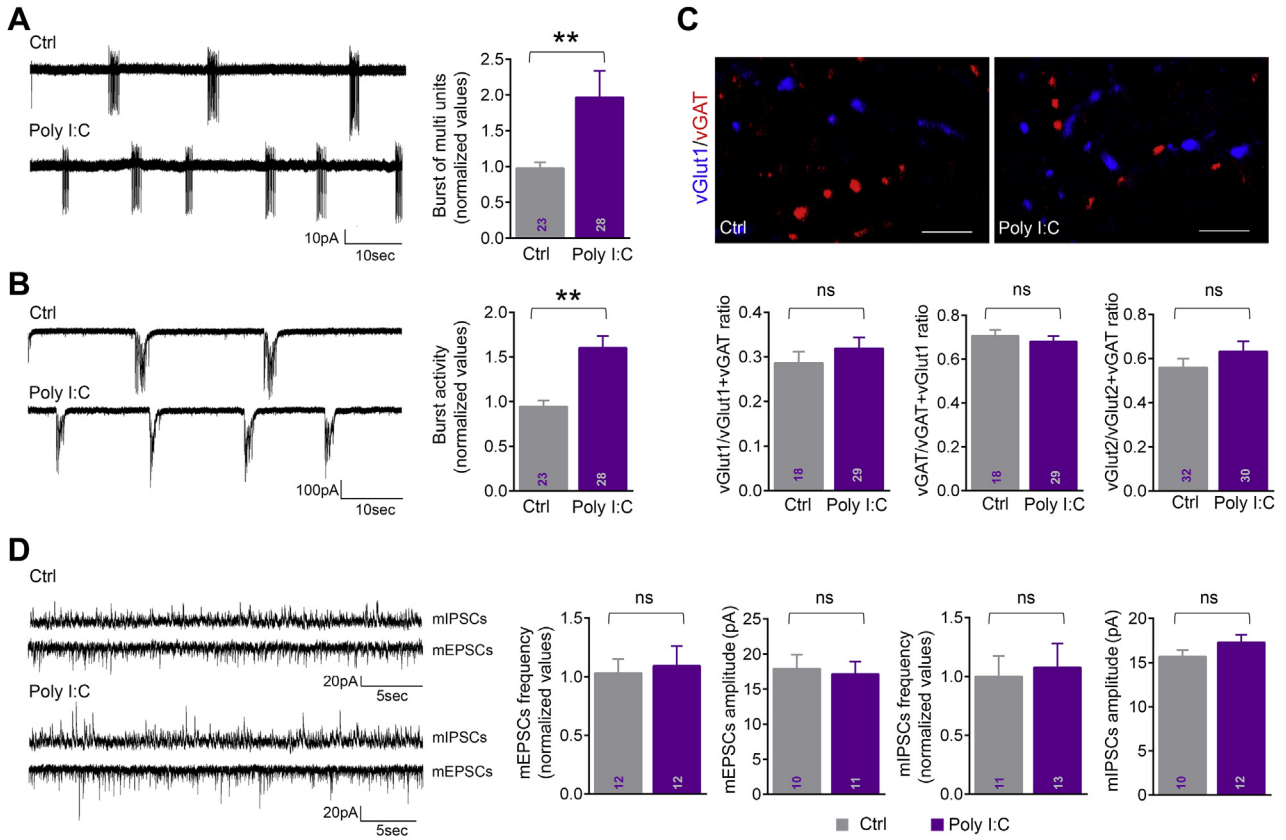

Figure 3. Primary hippocampal neurons from polyinosinic:polycytidylic acid (PolyI:C)–exposed embryos display altered burst activity. **(A)** (Left) Representative traces of cell-attached recording of spontaneous activity in control and PolyI:C–cultured neurons. (Right) Quantitative analysis of spontaneous activity shows a higher neuronal activity in 14 days in vitro (DIV) PolyI:C cultures compared with controls (Ctrls). Bars represent mean ± SEM (Ctrl = 0.98 ± 0.08, PolyI:C = 1.97 ± 0.37). Student's *t* test, $^{**}p < .01$. Numbers in bars indicate the number of cells. **(B)** (Left) Representative traces of bursts of action potentials in PolyI:C and Ctrl cultured neurons. (Right) Quantitative analysis of the burst activity recorded in 14 DIV primary cortical neurons showing a higher frequency of long bursts of action potentials in PolyI:C cultures. Bars represent mean ± SEM (Ctrl = 0.94 ± 0.07, PolyI:C = 1.60 ± 0.13). Student's *t* test, $^{**}p < .01$. Numbers in bars indicate the number of cells. **(C)** (Top) Representative immunofluorescence images obtained from 14 DIV primary cortical cultures established from embryos at embryonic day 18 that were prenatally treated with PolyI:C or vehicle showing the presynaptic excitatory marker vesicular glutamate transporter 1 (vGlut1) (in blue) and the presynaptic inhibitory marker vesicular gamma-aminobutyric acid transporter (vGAT) (in red) (scale bar = 5 μm). (Bottom) Quantitative analysis of the number of positive vGlut1/vGlut2 and vGAT puncta over the total number of vGlut1 + vGAT or vGlut2 + vGAT positive puncta showing no differences between the two experimental groups. Student's *t* test. Numbers in bars indicate the number of analyzed fields. **(D)** (Left) Representative traces of miniature excitatory postsynaptic currents (mEPSCs) and miniature inhibitory postsynaptic currents (mIPSCs) recorded in 14 DIV primary cortical neurons from prenatally treated embryos (PolyI:C or Ctrls). (Right) Electrophysiological analysis of the frequency and the amplitude of EPSCs and IPSCs showing no differences between the two experimental groups. Bars represent mean ± SEM (mEPSC frequency: Ctrl = 1.03 ± 0.12, PolyI:C = 1.09 ± 0.17; mEPSC amplitude: Ctrl = 17.92 ± 1.99, PolyI:C = 17.17 ± 1.74; mIPSC frequency: Ctrl = 1.00 ± 0.17, PolyI:C = 1.08 ± 0.20; mIPSC amplitude: Ctrl = 15.69 ± 0.73, PolyI:C = 17.31 ± 0.84). Student's *t* test. Numbers in bars indicate the number of cells. ns, not significant.

amoeboid appearance (29,30), in prenatally exposed brains, microglia displayed ramifications of comparable length, although slightly reduced in number, compared with controls (Supplemental Figure S2B). Also, the levels of cytokines IL-1β, IL-6, and tumor necrosis factor alpha, analyzed by real-time PCR, were under detection levels (not shown).

Seizures may also be the result of a change in the excitatory/inhibitory balance (31). We therefore investigated whether prenatal immune challenge altered glutamatergic or gamma-aminobutyric acidergic (GABAergic) synaptic transmission in the adult offspring. No differences were observed in either glutamatergic or GABAergic spontaneous synaptic currents in patch clamp recordings from P20 acute cortical slices from PolyI:C- or vehicle-exposed offspring: the frequency and amplitude of miniature excitatory postsynaptic currents and miniature inhibitory postsynaptic currents were comparable (Figure 1C). Consistently, Western blot analysis of E17 and P90 cortices from PolyI:C or control mice revealed no differences in the expression of synaptic markers, including the vesicular glutamate transporters vGlut1 and vGlut2, the GABA vesicular transporter vGAT, and the two soluble *N*-ethylmaleimide-sensitive factor attachment protein receptors SNAP-25 and syntaxin 1A (Supplemental Figure S3). These data indicate that the increased susceptibility to seizures of PolyI:C offspring is unlikely to result from imbalance in the relative number of excitatory or inhibitory synapses.

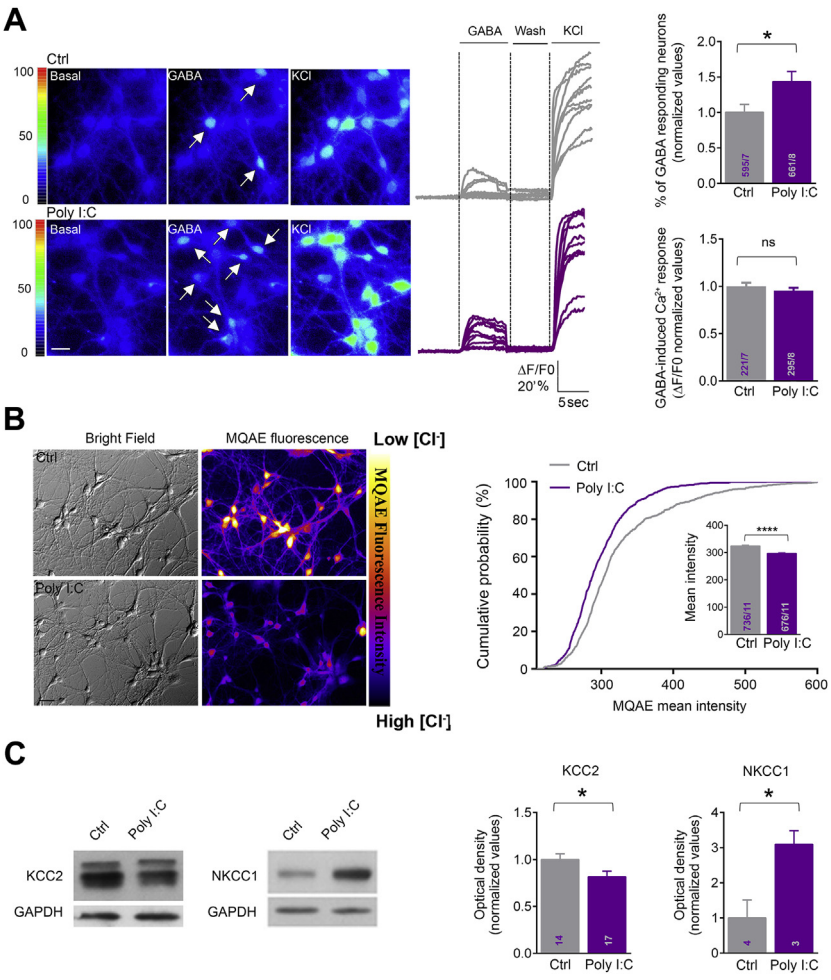

Figure 4. Primary hippocampal neurons from polyinosinic:polycytidylic acid (PolyI:C)–exposed embryos display altered excitatory-to-inhibitory switch. **(A)** (Left) Representative fluorescence images of 6 days in vitro cortical neurons loaded with the calcium dye Fura2 in basal state (left) and upon gamma-aminobutyric acid (GABA) (center) and KCl (right) stimulation; also shown are the temporal analyses of the respective calcium changes. White arrows indicate GABA-responding neurons. The quantitative analysis (right panels) shows a higher percentage of GABA-responding neurons in PolyI:C compared to control (Ctrl) cultures (top), whereas the magnitude of the GABA-induced calcium response was unchanged in the two conditions (bottom). Bars represent mean ± SEM (% of GABA-responding neurons: Ctrl = 1.00 ± 0.11, PolyI:C = 1.43 ± 0.14; GABA-induced calcium response [DF/F0]: Ctrl = 0.99 ± 0.04, PolyI:C = 0.95 ± 0.03). Student's *t* test, $*p < .05$ (scale bar = 40 μm). **(B)** (Left) Bright-field (left panels) and pseudocolor (right panels) images of *N*-(ethoxycarbonylmethyl)-6-methoxyquinolinium bromide (MQAE)–loaded neurons in the two experimental conditions. (Right) Cumulative probability and quantitative analysis of MQAE fluorescence indicate a significantly lower fraction of low-$[Cl^-]_i$ (high MQAE) cortical neurons in PolyI:C compared with Ctrls. Bars represent mean ± SEM (Ctrl = 324.3 ± 2.54, PolyI:C = 297.2 ± 1.65). Mann-Whitney *U* test, $****p < .0001$. Numbers in bars indicate the number of cells/animals. **(C)** K^+-Cl^- cotransporter 2 (KCC2) and Na^+-K^+-$2Cl^-$ cotransporter 1 (NKCC1) expression pattern in 6 days in vitro cortical cultures established from control and PolyI:C embryos. Student's *t* test, $*p < .05$. Numbers in bars indicate the number of embryos. ns, not significant.

Enhanced Excitation Is Associated With Defective Excitatory-to-Inhibitory Switch and Altered KCC2/NKCC1 Expression in PolyI:C Mice

A hyperactivity of neuronal networks may also result from a reduced inhibitory action of GABA, a phenomenon that might be linked to an altered excitatory-to-inhibitory switch. The latter process, which consists in the transition of GABA signaling from depolarizing to hyperpolarizing, starts soon after birth and is complete in rodents by the end of the first postnatal week. Defects in excitatory-to-inhibitory switch may lead to an excitatory/inhibitory imbalance (32,33). To assess whether the process of excitatory-to-inhibitory switch was correctly completed in PolyI:C cortical circuits, neurons were stimulated with a puff of 200-μM GABA, and spontaneous activity was recorded in cell-attached configuration. In contrast to control brain slices, where neuronal activity was slightly reduced by GABA application, GABA significantly increased the neuronal firing rate in PolyI:C slices (Figure 2A), indicating that the neurotransmitter still exerts an excitatory action in PolyI:C offspring. The resting potential of neurons was –65.88 ± 1.43 mV ($n = 8$) in control and –67.30 ± 1.36 mV ($n = 10$) in PolyI:C slices (unpaired *t* test, $p = .48$). Of note, application of the Na^+-K^+-$2Cl^-$ cotransporter 1 (NKCC1) antagonist bumetanide (10 μM) resulted in a significant reduction of spike frequency in PolyI:C slices (Figure 2B).

The excitatory action of GABA at early stages of neuronal development results from high intracellular chloride concentrations, which determine a more positive equilibrium potential for chloride and depolarizing chloride currents through $GABA_A$ receptors (34). In order to unequivocally demonstrate the occurrence of an altered excitatory-to-inhibitory switch in PolyI:C mouse brains, we directly monitored intracellular chloride levels ($[Cl^-]_i$) by means of fluorescence lifetime imaging microscopy of the chloride-sensitive dye *N*-(ethoxycarbonylmethyl)-6-methoxyquinolinium bromide (MQAE) in P20 brain slices. As expected, PolyI:C cortical slices showed a higher resting $[Cl^-]_i$ (revealed by a decrease in the fluorescence lifetime) compared with control mice (Figure 2C), indicating a delay in excitatory-to-inhibitory switch. Calibration measurement of MQAE lifetime with known intracellular chloride concentrations revealed a Stern–Volmer constant of 31 M^{-1} (Figure 2D). In the calibration experiments, control brain slices MQAE lifetime corresponded to

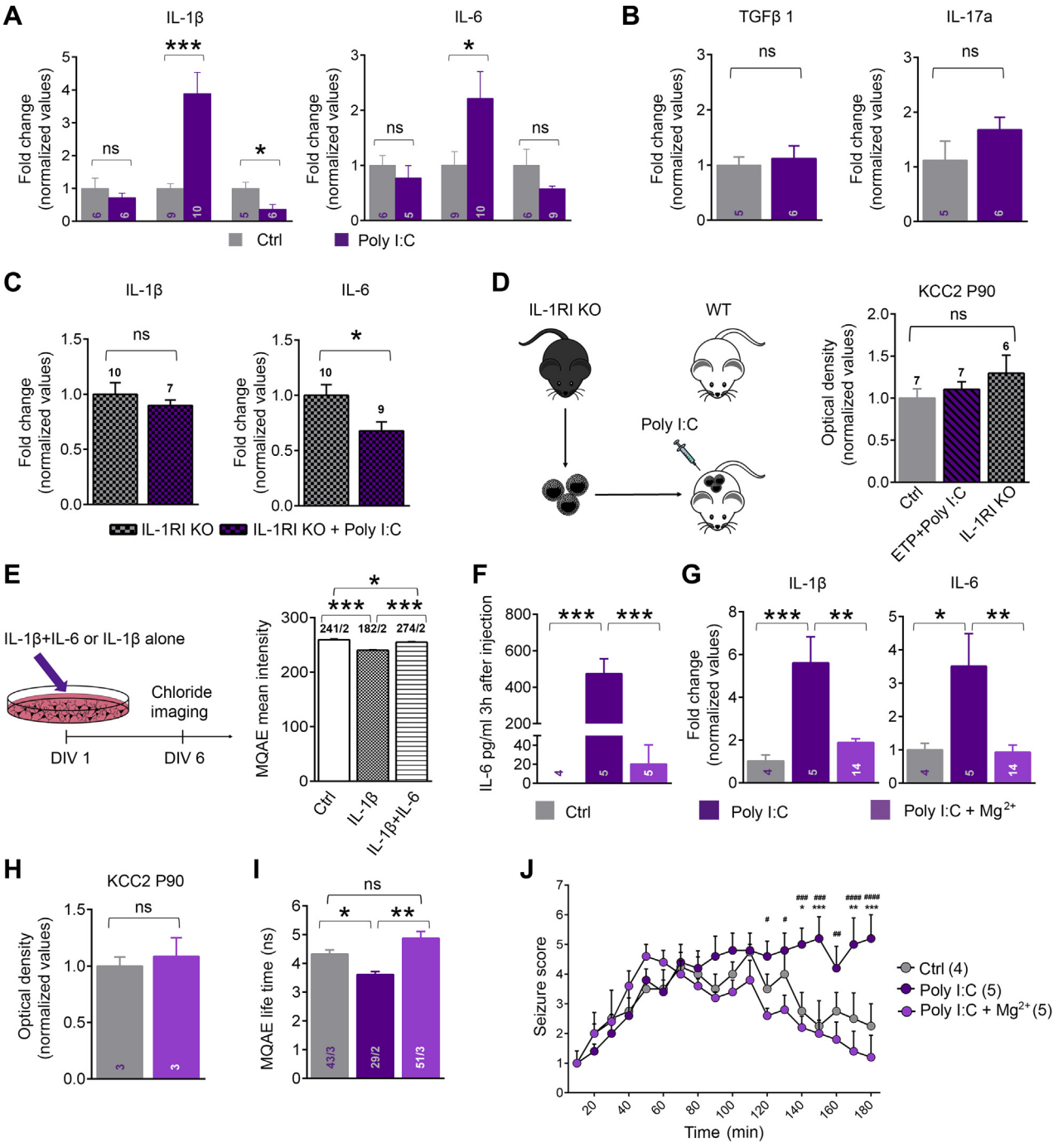

Figure 5. Magnesium sulfate prevents cytokine elevation in the embryos and reverts polyinosinic:polycytidylic acid (PolyI:C)–induced alterations. **(A)** Cytokine messenger RNA (mRNA) levels of interleukin-1β (IL-1β) and IL-6 in the embryos 3, 6, and 24 hours after vehicle or PolyI:C injection in the mother. Student's *t* test, $*p < .05$, $***p < .001$. Numbers in bars indicate the number of embryos. **(B)** Transforming growth factor-β (TGFβ1) and IL-17a in control (Ctrl) and PolyI:C prenatally treated embryos 6 hours after the injection in the mother. Numbers in bars indicate the number of embryos. **(C)** Embryonic mRNA levels of IL-1β and IL-6 six hours after the injection in interleukin-1 receptor type I knockout (IL-1RI KO) mothers showing no increase in cytokine mRNA upon PolyI:C administration. Numbers indicate the number of animals. **(D)** (Left) Schematic representation of embryo transfer procedure. (Right) Biochemical analysis of ion cotransporter K^+-Cl^- cotransporter 2 (KCC2) in Ctrls, embryo transfer procedure (ETP) offspring treated with PolyI:C, and naïve IL-1RI KO offspring at postnatal day 90 (P90) showing no increase in KCC2 expression in embryo transfer procedure offspring upon PolyI:C administration. Unchallenged IL-1RI KO mice were found to display higher, although not significantly, expression of KCC2. Numbers indicate the number of animals. **(E)** (Left) Scheme of primary neuronal cultures treatment with IL-1β alone (40 ng/mL) or in combination with IL-6 (10 ng/mL). (Right) Cortical neurons at 6 days in vitro (DIV) treated at 1 DIV with IL-1β alone or with IL-1β and IL-6 together display higher intracellular chloride levels as detected by *N*-(ethoxycarbonylmethyl)-6-methoxyquinolinium

an intracellular chloride concentration of 9.55 mM. Based on this estimate, chloride concentration in control brain slices turned out to be 9.5 ± 1.40 mM, whereas neurons in PolyI:C-treated slices displayed an intracellular chloride concentration of 15.4 ± 1.25 mM. Considering the extracellular concentration of chloride (139.2 mM), these values correspond to equilibrium potentials of –67.1 or –55.7 mV, for control and PolyI:C, respectively, and to driving forces for chloride ions of –1.1 and 10.2, respectively.

Chloride homeostasis in neurons is controlled through the developmentally regulated expression of NKCC1 (Cl^- importer) and KCC2 (Cl^- exporter) that undergo, respectively, a reduction (NKCC1) and a parallel increase (KCC2) during development, resulting in the switch from depolarizing to hyperpolarizing $GABA_A$ activation during neuronal maturation (32,33,35). Consistent with functional data, Western blotting analysis in homogenates from E17 and P20 cortices revealed a significantly higher expression of NKCC1 in PolyI:C versus control brains, which returned to control levels in adult P90 mice (Figure 2E). Conversely, both P20 and P90 PolyI:C cortices displayed a significantly lower KCC2 amount (Figure 2E). Therefore, a single challenge of the maternal immune system at GD9 delays the reciprocal changes in the expression of NKCC1 and KCC2, leading to higher intracellular chloride concentrations and delaying the disappearance of GABA excitatory activity.

The Neuronal Gene Repressor REST Displays Enhanced Binding to the KCC2 Promoter in PolyI:C Prenatally Exposed Mice

Real-time PCR was performed in P20 brains of PolyI:C- and vehicle-treated offspring (Figure 2A–C) to assess whether changes in mRNA levels accompanied the altered expression of KCC2 and NKCC1 observed at P20, the time point when our electrophysiological, fluorescence lifetime imaging microscopy–based, and Western blot experiments were performed. At difference with the decreased KCC2 and increased NKCC1 expression (Figure 2E), a change in relative mRNA levels was evident for KCC2 only (Figure 2F). Chromatin immunoprecipitation experiments were performed to get further insight into the processes responsible for reduced *Kcc2* transcription: we found increased binding of both REST (also known as neuron-restrictive silencer factor) and methyl-CpG-binding protein 2, which are known to repress *Kcc2* transcription (36), to position 509 of the *Kcc2* promoter (Figure 2G). These data indicate that prenatal PolyI:C activates epigenetic changes leading to the downregulation of *Kcc2* transcription and suggest that some posttranslational mechanisms may be responsible for the higher NKCC1 expression level.

PolyI:C-Induced Alterations Are Recapitulated in Neuronal Cultures

Our next goal was to investigate whether the altered excitatory-to-inhibitory switch promoted by maternal immune activation is a process intrinsically maintained in neurons independently from the brain environment. To specifically address this point, we established primary cultures of cortical neurons from embryos at E18 that were exposed to PolyI:C or vehicle at GD9. This selective analysis of neurons would rule out the possible contributions of other non-neuronal cell types. Spiking activity was assessed by multiunit recording, which reflects action potential firing in the cell attached mode (37). In line with ex vivo data, spontaneous spiking activity was significantly higher in PolyI:C neuronal cultures compared with controls (Figure 3A); spontaneous burst activity (38), which represents spontaneous paroxysmal depolarizing shifts due to synchronous neuronal firing (39,40), was also enhanced (Figure 3B). This occurred in the absence of changes in the density of vGlut1- or vGlut2-positive glutamatergic terminals or of vGAT-positive GABAergic terminals (Figure 3C); the frequency or amplitude of spontaneous miniature excitatory or miniature inhibitory postsynaptic currents (Figure 3D) were also unchanged, in line with the ex vivo experiments. The resting potential was –51.6 ± 0.99 mV (n = 17) in control and 52.2 ± 1.21 mV (n = 18) in PolyI:C-cultured neurons (unpaired t test, p = .70).

In line with GABA displaying depolarizing activity, cultures established from the brains of prenatally exposed offspring exhibited a higher percentage of neurons responding to GABA application with intracellular calcium elevations, as assessed by single-cell calcium imaging of cortical neurons loaded with the fluorescent dye Fura-2. The magnitudes of the calcium responses induced by GABA were not changed (Figure 4A). In agreement with the higher percentage of neurons responding to GABA (49% vs. 35%), the cumulative distribution of MQAE fluorescence intensity in PolyI:C versus control neuronal cultures revealed a higher average intracellular chloride level in PolyI:C neurons (Figure 4B). In particular, the percentages of neurons with MQAE readings <290 (high intracellular chloride) were about 49% for PolyI:C versus 35% for saline (consistent with the percentages of GABA-responding neurons); MQAE readings in these subpopulations were similarly distributed,

bromide (MQAE) fluorescence intensity reduction. One-way analysis of variance (ANOVA) followed by Tukey's multiple comparisons test, $^*p < .05$, $^{***}p < .001$. Numbers indicate the number of cells/animals. **(F)** Quantitative analysis of IL-6 plasmatic levels in adult female mice 3 hours after PolyI:C injection alone or with magnesium sulfate ($MgSO_4$) treatment before PolyI:C. $MgSO_4$ is able to prevent the increase in IL-6 plasma levels observed with the PolyI:C alone. Ordinary one-way ANOVA followed by Tukey's multiple comparisons test, $^{***}p < .001$. Numbers in bars indicate the number of animals. **(G)** Quantitative analysis of IL-1β and IL-6 mRNA levels in whole embryos 6 hours after vehicle, PolyI:C alone, or $MgSO_4$ + PolyI:C injection in the mother. $MgSO_4$ is able to prevent the increase in IL-1β and IL-6 mRNA levels observed in the PolyI:C embryos. One-way ANOVA followed by Tukey's multiple comparisons test, $^*p < .05$, $^{**}p < .01$, and $^{***}p < .001$. Numbers in bars indicate the number of embryos. **(H)** KCC2 protein levels in P90 offspring are not affected by PolyI:C prenatal treatment when $MgSO_4$ is administered before PolyI:C to the mother. Student's t test. Numbers in bars indicate the number of animals. **(I)** Quantitative analysis of intracellular chloride from fluorescence lifetime values measured by two-photon imaging in P20 brain slices. $MgSO_4$ can prevent the increase in $[Cl^-]_i$ observed in offspring prenatally treated with PolyI:C alone. Bars represent mean ± SEM (Ctrl = 4.32 ± 0.14, PolyI:C = 3.61 ± 0.10, $MgSO_4$ + PolyI:C = 4.87 ± 0.23). One-way ANOVA followed by Tukey's multiple comparisons test, $^*p < .05$, $^{**}p < .001$. **(J)** Time course of the behavioral response to 35 mg/kg kainic acid injection in Ctrl, PolyI:C, and $MgSO_4$ + PolyI:C offspring. Notably, $MgSO_4$ is able to prevent increased seizure susceptibility when administered in the mother before PolyI:C. One-way ANOVA followed by Sidak's multiple comparisons test, $^*p < .05$, $^{**}p < .01$, $^{***}p < .001$ (Ctrl vs. PolyI:C), $^{\#}p < .05$, $^{\#\#}p < .01$, $^{\#\#\#}p < .001$, $^{\#\#\#\#}p < .0001$ (PolyI:C vs. $MgSO_4$ + PolyI:C). Numbers in brackets indicate the number of animals. NS, not significant; WT, wild-type.

suggesting that neurons that had not switched yet had a similar distribution of intracellular chloride concentration; therefore, the similarly sized calcium responses to GABA were not unexpected. The change produced by PolyI:C in the expression pattern of the chloride cotransporters, KCC2 and NKCC1, was confirmed in cultured neurons: in 7 DIV PolyI:C cultures, neurons displayed lower levels of KCC2 and higher levels of NKCC1 (Figure 4C). These data indicate that the molecular consequences of an early immune challenge remain "sculpted" in the developmental program of neurons even when they are isolated from the brain environment.

Reducing Cytokine Elevation in the Embryo Is Sufficient to Avoid KCC2 Dysregulation

PolyI:C treatment, administered at GD9, is known to significantly increase IL-6 levels in the plasma of injected dams compared to vehicle treatment (6) (Supplemental Figure S1A). Of note, embryos from immune-challenged dams displayed a transient increase in the mRNA levels for the proinflammatory cytokines IL-1β and IL-6, which rose 6 hours after PolyI:C injection and returned to basal levels 24 hours after stimulation (Figure 5A). No differences were detected in the mRNA levels for transforming growth factor-β and IL-17a (Figure 5B).

To investigate whether the cytokine storm occurring in the offspring 6 hours after the dam challenge with PolyI:C could be at the origin of the dysregulation in transporter expression and in chloride homeostasis, we took advantage of IL-1RI KO mice, in which the immune response is subjected to a brake that tunes down the inflammatory process (41). As expected, differently from WT mice, PolyI:C injection in IL-1RI KO pregnant dams did not result in any elevation of IL-1β or IL-6 in the embryos (Figure 5C). To unequivocally dissect the contribution of the embryonic cytokines to the process, we performed an embryo transfer procedure: IL-1RI KO embryos were implanted in WT mothers, which would respond normally to PolyI:C treatment, the offspring alone being impaired in the immune activation process (Figure 5D, left). KCC2 expression levels were quantified at P90, when a high (around 30%) reduction of the transporter expression occurs in prenatally exposed WT mice (Figure 5D, right), and no changes of KCC2 were detected in the IL-1RI KO embryo transfer procedure offspring. Of note, unchallenged IL-1RI KO mice displayed higher expression of KCC2, suggesting an endogenous role of the immune response in controlling KCC2 expression, even under physiological conditions. In line with the role of cytokines in regulating neuronal developmental processes involved in chloride homeostasis, MQAE fluorescence intensity measurements indicated a higher intracellular chloride concentration in primary cortical neurons exposed to either a combination of IL-1β (40 ng/mL) and IL-6 (10 ng/mL) or to IL-1β alone (40 ng/mL) at 1 DIV and recorded at 6 DIV (Figure 5E).

Magnesium Sulfate Rescues PolyI:C-Induced Alterations

Given our demonstration that preventing cytokine elevation in the offspring brain is sufficient to prevent the subsequent reduction of KCC2 expression, we reasoned that pharmacological impairment of such increase could represent a good strategy to avoid possible neurodevelopmental defects after MIA. It has been reported that magnesium acts as an immunomodulator that is able to decrease inflammatory cytokine production (42). Of note, magnesium is already used to reduce inflammation at the maternal–fetal interface (43). We therefore investigated whether dam treatment with magnesium sulfate ($MgSO_4$) before PolyI:C injection (see Methods and Materials for details) prevented the increase of the proinflammatory cytokines. As expected, pretreated dams did not display elevations of IL-6 upon PolyI:C injection (Figure 5F). Accordingly, mRNA levels for IL-6 or IL-1β did not undergo any increase in embryos from $MgSO_4$-pretreated dams (Figure 5G). Consistent with our demonstration that preventing the cytokine elevations in the embryos is sufficient to prevent the transporter dysregulation, KCC2 expression was unaltered in the offspring of PolyI:C dams pretreated with $MgSO_4$ (Figure 5H). Consistently, the fluorescence lifetime imaging microscopy experiment indicated that intracellular chloride levels in P20 brain slices were comparable to those of vehicle-exposed offspring (Figure 5I; chloride concentration was estimated to 7.7 ± 1.16 mM in $MgSO_4$-pretreated PolyI:C animal slices vs. 9.5 ± 0.87 mM in control brain slices) and, even more importantly, the increased susceptibility to seizures was fully prevented (Figure 5J). These data indicate that $MgSO_4$ in the embryos can abolish the PolyI:C-dependent increase in proinflammatory cytokines and the long-lasting effects associated with MIA.

DISCUSSION

The use of mouse models based on prenatal immune activation allows for monitoring the impact of the challenge during development and is essential for determining the molecular pathways that mediate the resulting neuropathology (5,7,9). As underlined by Estes and McAllister (4), rodent models of MIA meet all the criteria for a valid disease model because they efficiently mimic a known disease-related risk factor (construct validity), exhibit a range of disease-related symptoms (face validity), and are effectively used to predict the efficacy of treatments (predictive validity). Despite these advantages, in most cases the mechanistic basis remains elusive.

Our study provides the demonstration that a single intrauterine exposure at GD9 significantly increases offspring susceptibility to seizures, drastically confining the temporal window of the detrimental immune hit; this contrasts with previous studies in which PolyI:C was administered daily during pregnancy (44). The neuronal network hyperactivity occurs in the absence of a classic inflammatory response in the offspring. Also, we did not find significant alterations in synapse pattern or spontaneous neurotransmission in offspring brain slices.

Which, then, is the molecular mechanism responsible for the network hyperexcitability in prenatally challenged mice? Our data indicate that MIA delays the normal developmental expression of KCC2, resulting in persistence of higher intracellular chloride concentrations and delayed GABA switch. Our study also unveils a molecular trajectory activated by MIA—i.e., the enhanced binding of the two repressors REST (also known as neuron-restrictive silencer factor) and methyl-CpG-binding protein 2 to the 509 site of the *Kcc2* promoter, which leads to reduced *Kcc2* transcription (36,45). Although NKCC1 expression is also altered, and higher levels were

observed in E17 and P20 PolyI:C offspring brains compared with controls, mRNA levels were not changed. Therefore, the reciprocal regulation of the two transporters is impaired at the transcriptional level for KCC2 and at the posttranslational level for NKCC1. Because of this imbalance, intracellular chloride concentrations are more elevated in PolyI:C offspring brain, and GABA persists in being excitatory at developmental time windows when it is normally inhibitory. This process renders neuronal networks hyperexcitable and susceptible to seizures triggered by excitatory stimuli. Genetic alterations in the *KCC2* gene have been reported to confer increased seizure susceptibility (46–51), but this is the first demonstration that an environmental stimulus can modify KCC2 expression and lead to an epileptic phenotype. Of note, a defect in depolarizing to hyperpolarizing switch, responsible for an excitatory/inhibitory imbalance, has been identified as a key pathophysiological mechanism not only in epilepsy but also in neurodevelopmental disorders, such as autism (52,53), which are typically associated with MIA and for which a mechanistic frame is still completely lacking. Consistent with a role for epigenetic mechanisms in changing the neuron developmental trajectories, the delay in excitatory-to-inhibitory switch is intrinsically maintained in neurons isolated from the brain and maintained in primary cultures, independently of the brain environment. This is consistent with behavioral alterations caused by MIA occurring in the first- and second-generation offspring of immune-challenged ancestors, demonstrating the transgenerational nongenetic inheritance of pathological traits (17).

We did not detect alterations in the activation profile of microglia in the adult offspring, in line with previous studies where no overt glial anomalies were detected in mice prenatally exposed to PolyI:C at either early or late stages of pregnancy (54,55). The transient increase in proinflammatory cytokines occurring in the fetal brain after MIA likely is at the root of the processes leading to KCC2 dysregulation. Indeed, normal expression of KCC2 in the offspring can be restored by genetic (IL-1RI KO) or pharmacological ($MgSO_4$) approaches able to prevent the transient increase in IL-6 and IL-1β in the fetal brain. Although we are presently unable to selectively pinpoint which one of the two cytokines—which are potently cross-regulated—may be directly responsible for the defective excitatory-to-inhibitory switch, it is notable that IL-1β is per se sufficient to alter chloride concentrations when applied to primary neuronal cultures, suggesting that this cytokine may be at the root of the process. It was recently suggested that immune signaling in neurons may converge upon mammalian target of rapamycin, which acts as a regulatory hub integrating inputs from numerous upstream intracellular signalling pathways, many of which are altered in the brains of immune-challenged offspring (4). Consistently, IL-1β impinges on the mammalian target of rapamycin/protein kinase B pathway, eventually impacting brain plasticity processes (56). Of note, a selective increase of IL-1β levels was detected in the hippocampi of GD9 PolyI:C-treated offspring, further pointing to a crucial role of this cytokine (55).

We finally suggest a translational exploitation of our findings that might be particularly profitable given the association between maternal infection during pregnancy and childhood epilepsy (57). $MgSO_4$, which has been previously shown to decrease the inflammatory cytokine production from immune cells (42), is able to fully prevent the increase of IL-6 and IL-1β in the brain of prenatally exposed mice, similar to what occurs in IL-1RI KO embryos. As a result, upon treatment of pregnant dams with $MgSO_4$, PolyI:C completely fails in causing KCC2 alterations and enhanced susceptibility to seizures. $MgSO_4$ can therefore be an early and relatively safe prevention treatment to avoid the long-term consequences of prenatal infections. Although magnesium is already used in clinics to reduce inflammation at the maternal–fetal interface under specific pathological conditions (43), the protocols for the use of $MgSO_4$ remain controversial. Aside from ideal dosing and timing remaining unclear, "the different gestational ages at randomization leave clinicians confused about which patients should be candidates for neuroprotection" (58). Our data clearly indicate a key time window (the end of the first trimester of pregnancy, i.e., the beginning of cortical layering) in which maternal treatment with $MgSO_4$ may be decisive for preventing disturbances to one of the most relevant neurodevelopmental mechanisms, the GABA developmental switch. In this frame, $MgSO_4$ may be proposed as a safe therapeutic intervention to decrease the incidence of immune-mediated neurological or psychiatric illness in adulthood caused by maternal viral infections at the end of the first trimester of pregnancy.

ACKNOWLEDGMENTS AND DISCLOSURES

This work was supported by Ministero della Salute Grant No. GR-2011-02347377, Cariplo Grant No. 2015-0594, Fondazione Vodafone, and Humanitas institutional funding (to MM), Cariplo Grant No. 2014-0655 (to IB, MM), and by Cariplo Grant No. 2015-0952 (to RT). IC is supported by a Fondazione Giancarla Vollaro Fellowship. RT was previously supported by a Fondazione Umberto Veronesi Fellowship. The financial support of Fondazione Telethon-Italy Grant No. GGP16015 (to FA) is acknowledged. FA was previously supported by the Italian Ministry of Research and Education program "FIRB Giovani" 2010 (Grant No. RBFR10ZBYZ).

We thank the Monzino Foundation (Milan, Italy) for its generous gift of the LSM 510 Meta confocal microscope.

The authors report no biomedical financial interests or potential conflicts of interest.

ARTICLE INFORMATION

From the Istituto di Ricovero e Cura a Carattere Scientifico Humanitas (IC, MR, RM, GD, RT, ML, EG, DM, DP, MM) and Hunimed University (MR, RF, IB, DP), Rozzano; Institute of Neuroscience - National Research Council (IC, EF, MM), Department of Biotechnology and Translational Medicine, University of Milan (EF, EG, FA), University of Milano-Bicocca (GD), and Institute for Genetic and Biomedical Research - National Research Council (ML), Milan; and the Neuroscience Center (RF), Dipartimento di Scienze Teoriche e Applicate, Insubria University, Busto Arsizio, Italy.

IC and EF contributed equally to this work.

Address correspondence to Michela Matteoli, Ph.D., Istituto di Neuroscienze Consiglio Nazionale delle Ricerche, via Vanvitelli 32, 20129 Milano, Italy; E-mail: m.matteoli@in.cnr.it; michela.matteoli@humanitasresearch.it.

Received Apr 26, 2017; revised Aug 3, 2017; accepted Sep 11, 2017.

Supplementary material cited in this article is available online at https://doi.org/10.1016/j.biopsych.2017.09.030.

REFERENCES

1. Scola G, Duong A (2017): Prenatal maternal immune activation and brain development with relevance to psychiatric disorders. Neuroscience 346:403–408.
2. Knuesel I, Chicha L, Britschgi M, Schobel SA, Bodmer M, Hellings JA, *et al.* (2014): Maternal immune activation and abnormal brain development across CNS disorders. Nat Rev Neurol 10:643–660.

3. Meyer U (2014): Prenatal poly(i:C) exposure and other developmental immune activation models in rodent systems. Biol Psychiatry 75: 307–315.
4. Estes ML, McAllister AK (2016): Maternal immune activation: Implications for neuropsychiatric disorders. Science 353:772–777.
5. Meyer U, Feldon J, Schedlowski M, Yee BK (2006): Immunological stress at the maternal-foetal interface: A link between neurodevelopment and adult psychopathology. Brain Behav Immun 20: 378–388.
6. Meyer U, Nyffeler M, Engler A, Urwyler A, Schedlowski M, Knuesel I, *et al.* (2006): The time of prenatal immune challenge determines the specificity of inflammation-mediated brain and behavioral pathology. J Neurosci 26:4752–4762.
7. Fatemi SH, Reutiman TJ, Folsom TD, Huang H, Oishi K, Mori S, *et al.* (2008): Maternal infection leads to abnormal gene regulation and brain atrophy in mouse offspring: implications for genesis of neurodevelopmental disorders. Schizophr Res 99:56–70.
8. Fortier ME, Luheshi GN, Boksa P (2007): Effects of prenatal infection on prepulse inhibition in the rat depend on the nature of the infectious agent and the stage of pregnancy. Behav Brain Res 181:270–277.
9. da Silveira VT, Medeiros DC, Ropke J, Guidine PA, Rezende GH, Moraes MF, *et al.* (2017): Effects of early or late prenatal immune activation in mice on behavioral and neuroanatomical abnormalities relevant to schizophrenia in the adulthood. Int J Dev Neurosci 58:1–8.
10. Harvey L, Boksa P (2012): Prenatal and postnatal animal models of immune activation: Relevance to a range of neurodevelopmental disorders. Dev Neurobiol 72:1335–1348.
11. Shi L, Fatemi SH, Sidwell RW, Patterson PH (2003): Maternal influenza infection causes marked behavioral and pharmacological changes in the offspring. J Neurosci 23:297–302.
12. Meyer U, Feldon J, Schedlowski M, Yee BK (2005): Towards an immuno-precipitated neurodevelopmental animal model of schizophrenia. Neurosci Biobehav Rev 29:913–947.
13. Hava G, Vered L, Yael M, Mordechai H, Mahoud H (2006): Alterations in behavior in adult offspring mice following maternal inflammation during pregnancy. Dev Psychobiol 48:162–168.
14. Golan HM, Lev V, Hallak M, Sorokin Y, Huleihel M (2005): Specific neurodevelopmental damage in mice offspring following maternal inflammation during pregnancy. Neuropharmacology 48:903–917.
15. Stolp HB, Turnquist C, Dziegielewska KM, Saunders NR, Anthony DC, Molnar Z (2011): Reduced ventricular proliferation in the foetal cortex following maternal inflammation in the mouse. Brain 134(pt 11): 3236–3248.
16. Ellman LM, Deicken RF, Vinogradov S, Kremen WS, Poole JH, Kern DM, *et al.* (2010): Structural brain alterations in schizophrenia following fetal exposure to the inflammatory cytokine interleukin-8. Schizophr Res 121:46–54.
17. Weber-Stadlbauer U, Richetto J, Labouesse MA, Bohacek J, Mansuy IM, Meyer U (2017): Transgenerational transmission and modification of pathological traits induced by prenatal immune activation. Mol Psychiatry 22:102–112.
18. Gyorffy BA, Gulyassy P, Gellen B, Volgyi K, Madarasi D, Kis V, *et al.* (2016): Widespread alterations in the synaptic proteome of the adolescent cerebral cortex following prenatal immune activation in rats. Brain Behav Immun 56:289–309.
19. Behringer R, Gertsenstein M, Vintersten Nagy K, Nagy A (2003): Manipulating the Mouse Embryo: A Laboratory Manual, 3rd ed. Cold Spring Harbor, NY: Cold Spring Harbor Laboratory Press.
20. Hallak M, Kupsky WJ, Hotra JW, Evans JB (1999): Fetal rat brain damage caused by maternal seizure activity: Prevention by magnesium sulfate. Am J Obstet Gynecol 181:828–834.
21. Pozzi D, Condliffe S, Bozzi Y, Chikhladze M, Grumelli C, Proux-Gillardeaux V, *et al.* (2008): Activity-dependent phosphorylation of Ser187 is required for SNAP-25-negative modulation of neuronal voltage-gated calcium channels. Proc Natl Acad Sci U S A 105: 323–328.
22. Racine RJ (1972): Modification of seizure activity by electrical stimulation. II. Motor seizure. Electroencephalogr Clin Neurophysiol 32: 281–294.
23. Pozzi D, Lignani G, Ferrea E, Contestabile A, Paonessa F, D'Alessandro R, *et al.* (2013): REST/NRSF-mediated intrinsic homeostasis protects neuronal networks from hyperexcitability. EMBO J 32:2994–3007.
24. Antonucci F, Corradini I, Morini R, Fossati G, Menna E, Pozzi D, *et al.* (2013): Reduced SNAP-25 alters short-term plasticity at developing glutamatergic synapses. EMBO Rep 14:645–651.
25. Pizzamiglio L, Focchi E, Murru L, Tamborini M, Passafaro M, Menna E, *et al.* (2016): New role of ATM in controlling GABAergic tone during development. Cereb Cortex 26:3879–3888.
26. Verderio C, Coco S, Fumagalli G, Matteoli M (1994): Spatial changes in calcium signaling during the establishment of neuronal polarity and synaptogenesis. J Cell Biol 126:1527–1536.
27. Lein PJ, Barnhart CD, Pessah IN (2011): Acute hippocampal slice preparation and hippocampal slice cultures. Methods Mol Biol 758:115–134.
28. Maroso M, Balosso S, Ravizza T, Liu J, Aronica E, Iyer AM, *et al.* (2010): Toll-like receptor 4 and high-mobility group box-1 are involved in ictogenesis and can be targeted to reduce seizures. Nat Med 16:413–419.
29. Ransohoff RM, Perry VH (2009): Microglial physiology: Unique stimuli, specialized responses. Ann Rev Immunol 27:119–145.
30. Hanisch UK, Kettenmann H (2007): Microglia: Active sensor and versatile effector cells in the normal and pathologic brain. Nat Neurosci 10:1387–1394.
31. Bradford HF (1995): Glutamate, GABA and epilepsy. Prog Neurobiol 47:477–511.
32. Ben-Ari Y, Cherubini E, Corradetti R, Gaiarsa JL (1989): Giant synaptic potentials in immature rat CA3 hippocampal neurones. J Physiol 416:303–325.
33. Valeeva G, Valiullina F, Khazipov R (2013): Excitatory actions of GABA in the intact neonatal rodent hippocampus in vitro. Front Cell Neurosci 7:20.
34. Ben-Ari Y (2002): Excitatory actions of gaba during development: The nature of the nurture. Nat Rev Neurosci 3:728–739.
35. Cherubini E, Gaiarsa JL, Ben-Ari Y (1991): GABA: An excitatory transmitter in early postnatal life. Trends Neurosci 14:515–519.
36. Yeo M, Berglund K, Augustine G, Liedtke W (2009): Novel repression of Kcc2 transcription by REST-RE-1 controls developmental switch in neuronal chloride. J Neurosci 29:14652–14662.
37. Logothetis NK (2003): The underpinnings of the BOLD functional magnetic resonance imaging signal. J Neurosci 23:3963–3971.
38. Robinson HP, Kawahara M, Jimbo Y, Torimitsu K, Kuroda Y, Kawana A (1993): Periodic synchronized bursting and intracellular calcium transients elicited by low magnesium in cultured cortical neurons. J Neurophysiol 70:1606–1616.
39. Rohrbacher J, Jarolimek W, Lewen A, Misgeld U (1997): GABAB receptor-mediated inhibition of spontaneous inhibitory synaptic currents in rat midbrain culture. J Physiology 500(pt 3):739–749.
40. Li YX, Zhang Y, Lester HA, Schuman EM, Davidson N (1998): Enhancement of neurotransmitter release induced by brain-derived neurotrophic factor in cultured hippocampal neurons. J Neurosci 18:10231–10240.
41. Glaccum MB, Stocking KL, Charrier K, Smith JL, Willis CR, Maliszewski C, *et al.* (1997): Phenotypic and functional characterization of mice that lack the type I receptor for IL-1. J Immunol 159: 3364–3371.
42. Sugimoto J, Romani AM, Valentin-Torres AM, Luciano AA, Ramirez Kitchen CM, Funderburg N, *et al.* (2012): Magnesium decreases inflammatory cytokine production: A novel innate immunomodulatory mechanism. J Immunol 188:6338–6346.
43. Dowling O, Chatterjee PK, Gupta M, Tam Tam HB, Xue X, Lewis D, *et al.* (2012): Magnesium sulfate reduces bacterial LPS-induced inflammation at the maternal-fetal interface. Placenta 33:392–398.
44. Pineda E, Shin D, You SJ, Auvin S, Sankar R, Mazarati A (2013): Maternal immune activation promotes hippocampal kindling epileptogenesis in mice. Ann Neurol 74:11–19.
45. Yeo M, Berglund K, Hanna M, Guo JU, Kittur J, Torres MD, *et al.* (2013): Bisphenol A delays the perinatal chloride shift in cortical

neurons by epigenetic effects on the Kcc2 promoter. Proc Natl Acad Sci U S A 110:4315–4320.

46. Hekmat-Scafe DS, Lundy MY, Ranga R, Tanouye MA (2006): Mutations in the K+/Cl- cotransporter gene kazachoc (kcc) increase seizure susceptibility in Drosophila. J Neurosci 26:8943–8954.
47. Woo NS, Lu J, England R, McClellan R, Dufour S, Mount DB, *et al.* (2002): Hyperexcitability and epilepsy associated with disruption of the mouse neuronal-specific K-Cl cotransporter gene. Hippocampus 12:258–268.
48. Buchin A, Chizhov A, Huberfeld G, Miles R, Gutkin BS (2016): Reduced efficacy of the KCC2 cotransporter promotes epileptic oscillations in a subiculum network model. J Neurosci 36:11619–11633.
49. Robinson S, Mikolaenko I, Thompson I, Cohen ML, Goyal M (2010): Loss of cation-chloride cotransporter expression in preterm infants with white matter lesions: Implications for the pathogenesis of epilepsy. J Neuropathol Exp Neurol 69:565–572.
50. Puskarjov M, Seja P, Heron SE, Williams TC, Ahmad F, Iona X, *et al.* (2014): A variant of KCC2 from patients with febrile seizures impairs neuronal Cl- extrusion and dendritic spine formation. EMBO Rep 15:723–729.
51. Kahle KT, Merner ND, Friedel P, Silayeva L, Liang B, Khanna A, *et al.* (2014): Genetically encoded impairment of neuronal KCC2 cotransporter function in human idiopathic generalized epilepsy. EMBO Rep 15:766–774.
52. Cellot G, Cherubini E (2014): GABAergic signaling as therapeutic target for autism spectrum disorders. Front Pediatr 2:70.
53. Sgado P, Dunleavy M, Genovesi S, Provenzano G, Bozzi Y (2011): The role of GABAergic system in neurodevelopmental disorders: A focus on autism and epilepsy. Int J Physiol Pathophysiol Pharmacol 3: 223–235.
54. Giovanoli S, Notter T, Richetto J, Labouesse MA, Vuillermot S, Riva MA, *et al.* (2015): Late prenatal immune activation causes hippocampal deficits in the absence of persistent inflammation across aging. J Neuroinflammation 12:221.
55. Giovanoli S, Weber-Stadlbauer U, Schedlowski M, Meyer U, Engler H (2016): Prenatal immune activation causes hippocampal synaptic deficits in the absence of overt microglia anomalies. Brain Behav Immun 55:25–38.
56. Tomasoni R, Morini R, Lopez-Atalaya JP, Corradini I, Canzi A, Rasile M, *et al.* (2017): Lack of IL-1R8 in neurons causes hyperactivation of IL-1 receptor pathway and induces MECP2-dependent synaptic defects. Elife 6.
57. Norgaard M, Ehrenstein V, Nielsen RB, Bakketeig LS, Sorensen HT (2012): Maternal use of antibiotics, hospitalisation for infection during pregnancy, and risk of childhood epilepsy: A population-based cohort study. PloS One 7:e30850.
58. Chang E (2015): Preterm birth and the role of neuroprotection. BMJ 350:g6661.